



ChemComm

**Selective Sensing of THC and Related Metabolites in
Biofluids by Host:Guest Arrays**

Journal:	<i>ChemComm</i>
Manuscript ID	CC-COM-02-2020-001489.R1
Article Type:	Communication

SCHOLARONE™
Manuscripts

Selective Sensing of THC and Related Metabolites in Biofluids by Host:Guest Arrays

 Adam D. Gill,^b Briana L. Hickey,^a Wenwan Zhong^{a,c} and Richard J. Hooley^{a,b,*}

 Received 00th January 20xx,
 Accepted 00th January 20xx

DOI: 10.1039/x0xx00000x

www.rsc.org/

A water-soluble host molecule can bind tetrahydrocannabinol (Δ^9 -THC) and its metabolites in aqueous solution. By pairing this recognition event in a sensing array with fluorescent reporters and varying external mediators, pattern recognition-based detection is possible, which allows selective discrimination of the THC metabolites. The selective sensing can be performed in aqueous solution with micromolar sensitivity, as well as in biofluids such as urine and saliva. Metabolites as similar as Δ^8 - and Δ^9 -THC, differing only in the position of a double bond, can be distinguished.

Water-soluble synthetic host molecules¹ such as calixarenes,^{1a} cyclophanes,^{1b} cucurbiturils,^{1c} pillararenes^{1d} and deep cavitands^{1e} have seen a wide selection of applications in the molecular recognition and sensing of biologically important targets in recent years.² Exquisite selectivity and affinity has been shown for species as varied as steroids,^{3a} peptides^{3b-d} and proteins.^{3e} They are also highly amenable to array-based pattern recognition sensing, which allows even greater discrimination between molecules of similar structure.⁴ However, one of the main challenges remains their limited function in biological media, as opposed to simple buffered aqueous solution. Intracellular environments and biofluids such as saliva or urine all contain competing species that reduce target selectivity, limiting the effectiveness of host molecules for *in vivo* biosensing.⁵ There are examples of indicator displacement assays and selective molecular recognition in cells⁶ using calixarenes^{6a} or deep cavitands,^{6b} and cucurbiturils have shown affinity for cationic targets in biological media.⁷ Some hosts show good function in bodily fluids,⁸ such as the “DimerDye” calixarenes,⁹ which bind cationic species such as methylated lysine peptides^{9a} and alkaloid drugs^{9b} in urine and saliva. Recognition of neutral targets in biological media is much

more challenging, however, and more prone to interference by high concentrations of salt or urea in the complex milieu.

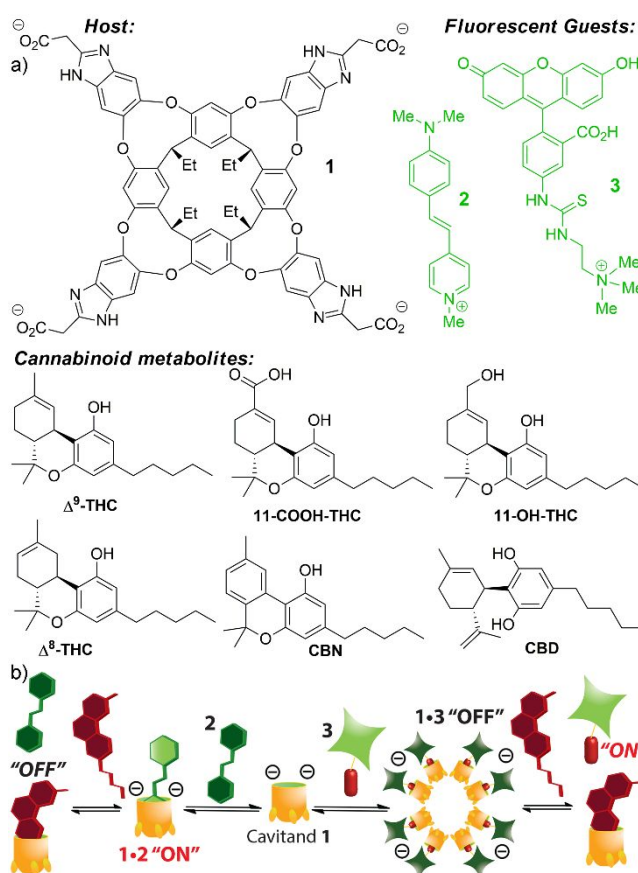


Figure 1. a) Sensor components used and cannabinoid target structures; b) an illustration of the various sensing mechanisms in the array.

An important example of a neutral target is tetrahydrocannabinol (Δ^9 -THC, Figure 1), the major psychoactive ingredient in marijuana. Once ingested, Δ^9 -THC is primarily metabolized to 11-OH-THC and subsequently oxidized to 11-COOH-THC before excretion from the body.¹⁰ Saliva concentrations of Δ^9 -THC are highest immediately following

^aDepartment of Chemistry; ^bDepartment of Biochemistry and Molecular Biology; ^cEnvironmental Toxicology Program; University of California-Riverside, Riverside, CA 92521, U.S.A.

* E-mail: richard.hooley@ucr.edu

Electronic Supplementary Information (ESI) available: Full fluorescence response and discriminant analysis data. See DOI: 10.1039/x0xx00000x

marijuana smoking, with values ranging from 8.4–71.2 μM , while urine concentrations of **11-COOH-THC** peak several hours after ingestion, with values up to 0.48 μM .^{10d-e} Sensing these molecules is not trivial for macrocyclic water-soluble hosts, as the targets are quite similar in structure and do not contain an easily recognizable “handle” for binding.

Most current methods of cannabinoid detection in bodily fluids rely on either immunoassays, or chromatography followed by mass spectrometry.¹⁰ Both methods have very low limits of detection but have important drawbacks: immunoassays often show poor discrimination between metabolites with analogous structures, and MS methods require extensive sample preparation and instrumentation.^{10a-b} A simple, selective optical sensor capable of structural discrimination in bodily fluids would be highly valuable.

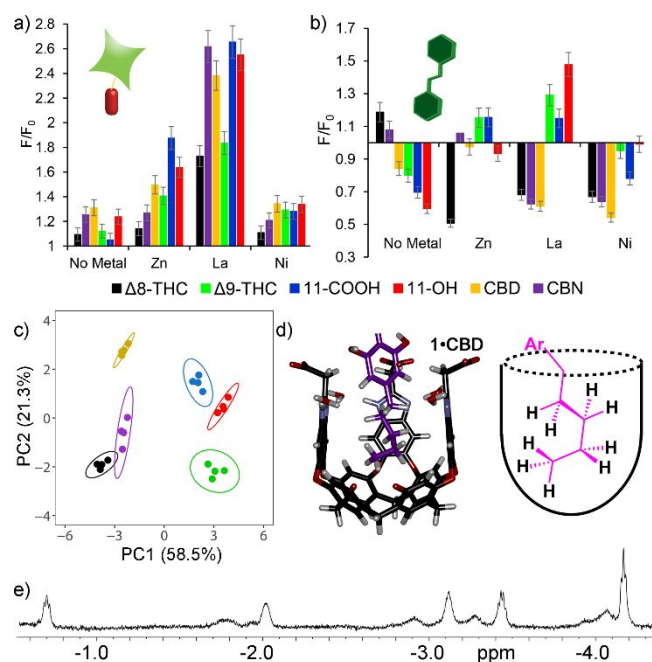


Figure 2. Fluorescence responses of the 6 different THC metabolites in buffered aqueous solution with a) guest **3**; b) guest **2**. [**1**] = 20 μM ; [**2**] = 1.5 μM ; [**3**] = 3 μM ; [M^{2+}] = 50 μM ; [THC metabolite] = 30 μM , 20 mM Tris buffer, pH = 7.4; c) 2D PCA scores plot from a 14 factor array with **1**•**2** or **1**•**3** and either no metal or 50 μM Zn²⁺, Cu²⁺, Co²⁺, Ni²⁺, Cd²⁺, La³⁺ or Ca²⁺. Ellipses determined at 95% confidence in RStudio. d) Minimized structure of the **1**•CBD complex, illustrating the helical conformation of the alkyl tail; e) upfield region of the ¹H NMR spectrum of **1**•CBD in D₂O (500 MHz, 298K).

Deep, self-folding cavitands such as **1** can provide a solution. This host shows strong (μM) affinity for *n*-alkanes and substituted hydrocarbons in water,¹¹ and has been widely used for sensing a variety of biomolecules in water,^{3d} cells^{6b} and urine.¹² Δ⁹-THC and its metabolites all contain an *n*-pentyl chain, which should be able to bind in the cavity of **1**, and pairing this recognition with a suitable dye partner for indicator displacement assays should allow optical sensing. Six cannabinoid targets were chosen for testing (Figure 1), including Δ⁹-THC and cannabidiol (CBD), the two major oxidative metabolites **11-COOH-THC** and **11-OH-THC**, and two analogs that are extremely similar in structure to Δ⁹-THC, Δ⁸-THC and cannabinol CBN. The challenge in selectively sensing these targets is that the major variations are in the ring

structures, not the *n*-pentyl chain. Fortunately, host **1** can be easily applied to a chemical nose-style arrayed sensing format: its recognition capabilities are highly dependent on fluorophore type and other environmental factors.^{3d,e}

The recognition abilities of host **1** were initially tested by indicator displacement assays of the six THC targets using two different fluorophores **2** and **3**, which are well-precedented for target sensing with **1**.^{3d,e} The **1**•**2/3** complexes ([**1**] = 20 μM) were treated with the six THC analogs in 20 mM Tris buffer at pH 7.4, in the presence of a suite of 7 heavy metal salts (50 μM), which have been previously shown to strongly coordinate to the upper rim carboxylates of **1**, modulating its affinity for different targets and allowing simple array-based sensing with only one or two host:guest components.¹³ The fluorescence responses are shown in Figures 2a and b (for full data, see ESI). Most obviously, the responses illustrate that host **1** does bind the THC analogs, displacing the dyes, and that the responses are indeed variable for each metabolite. The results from the full array were subjected to both Linear Discriminant Analysis (LDA) and Principal Component Analysis (PCA), which are biased and unbiased statistical discriminant methods respectively.¹⁴ The unbiased PCA scores plot for the six THC analogs is shown in Figure 2c, and shows the effectiveness of the sensing array: all six metabolites can be fully discriminated, even via the unbiased PCA method. 95% confidence ellipses are shown in the plot, and all the data points are fully discriminated at 95% confidence, with a slight overlap between the signal clusters for CBN and Δ⁹-THC. Most impressively, Δ⁹-THC and Δ⁸-THC are fully discriminated, despite only varying in structure by the position of a single C=C double bond. The LDA discrimination is even more impressive (see ESI), with full selectivity for all six targets possible even with a minimal array of 4 factors. The sensitivity of the array was also strong. Limits of detection (LOD) for the three primary cannabis metabolites (Δ⁹-THC, 11-OH-THC, and 11-COOH-THC) were calculated using the **1**•**3** host:guest complex, and determined to be 8.2 μM , 4.5 μM , and 17.4 μM respectively (Figure S-3).

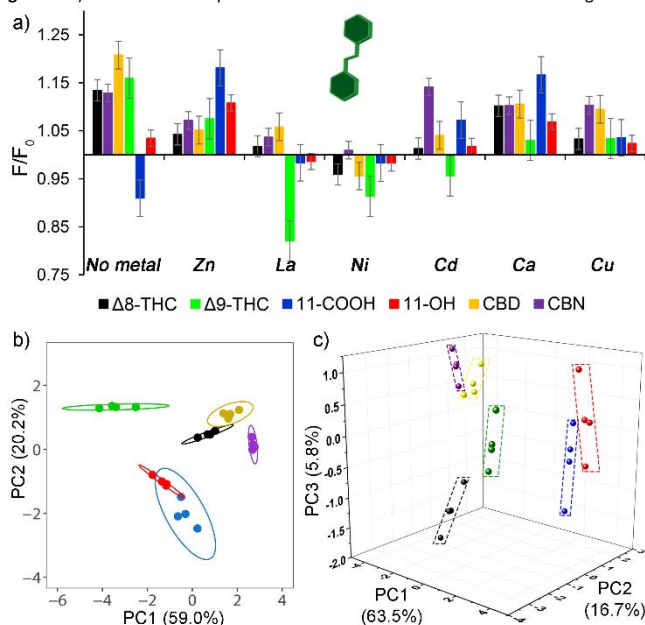
The selectivity in buffered aqueous solution is impressive, even more so when considering the method of host:target binding. ¹H NMR analysis was possible with CBD. The upfield region of the NMR spectrum illustrates that the *n*-pentyl chain of CBD binds inside the cavity, and coils into the expected helical conformation when bound (Figure 2e).¹⁵ Molecular modeling of the **1**•CBD complex shows that the aromatic ring resides close to the upper rim carboxylate groups and any bound metal ions. It is reasonable to suggest that changes in binding affinity are due to variable interactions between the upper rim functions of **1** and the ring systems of the bound targets. Even so, it is impressive that such small changes in structure, remote from the cavity, can be sensed with good selectivity.

The mechanisms of fluorescence response are more complex than simple displacement, however. Fluorescein guest **3** is known to trigger self-assembly of **1** into larger aggregates upon binding, causing self-quenching of the fluorophore (see Figure 1c for representative cartoon).^{3d} Competitive displacement of **3** by a target causes an increase in fluorescence, which is what is seen in Figure 2. The presence of metal ions causes additional

quenching of the bound fluorophore, and/or increased aggregation, depending on the nature of the metal.¹³ Either way, displacement of **3** from these complex host:guest assemblies by THC causes a fluorescence recovery. DMSI **2** shows a far more complex response with the different THC metabolites: some cause a fluorescence increase, some cause additional quenching. DMSI **2** itself shows enhanced fluorescence upon binding in **1**, so displacement should cause a drop in signal. The presence of metals (and triggered self-assembly and self-quenching) makes this simple indicator displacement process far more nuanced, however, and it is clear that multiple recognition mechanisms are occurring here.

The selective sensing of the THC metabolites in water is impressive, but hardly unexpected: these host:guest arrays can selectively sense many different target types with high fidelity.^{3d,12} To stretch the capabilities of the system, we tested it in biofluids: urine and saliva. Commercial marijuana tests use two types of detection method, either from a saliva sample, focusing on Δ^9 -THC, or a urine test that detects **11-COOH-THC**. We therefore repeated the fluorescence array tests, initially spiking the THC metabolites (30 μ M) into arrayed samples of host (20 μ M), fluorophore (1.5 or 3 μ M) and metals (50 μ M) into commercial samples of sterile human urine.

Figure 3. a) Fluorescence responses of the 6 different THC metabolites with guest **2** in



pooled human urine. b) 2D PCA scores plot from a 7-factor array using **1•2** and either no metal or 50 μ M Zn^{2+} , Cu^{2+} , Ni^{2+} , Cd^{2+} , La^{3+} or Ca^{2+} ; c) 3D PCA scores plot using the full 14-factor array with **1•2** or **1•3** and either no metal or 50 μ M Zn^{2+} , Cu^{2+} , Ni^{2+} , Cd^{2+} , La^{3+} or Ca^{2+} . [1] = 20 μ M; [2] = 1.5 μ M; [3] = 3 μ M; [M^{2+}] = 50 μ M; [THC metabolite] = 30 μ M. Ellipses determined at 95% confidence.

The fluorescence responses from the urine screen are shown in Figure 3a (with guest **2**) and in the ESI (with guest **3**). The immediate takeaway from the measurements is that the relative response changes are lower than in aqueous solution, which is to be expected, given the number of possible interferents in the solution. However, as can be seen in Figure 3a, the fluorescence signal variations for the different THC

metabolites are still present, especially for guest **2**. Further analysis of the signals shows that the **1•2** complex is far more effective in detecting the THC targets in urine than the fluorescein-based **1•3**. The PCA scores plot for the **1•2** sensor in the presence of six metals is shown in Figure 3b, and illustrates that a single host:fluorophore complex is capable of robust differentiation of most of the THC metabolites. There is very slight overlap in the 95% confidence intervals for **CBD** and Δ^8 -THC, and the more water-soluble metabolites **11-COOH-THC** and **11-OH-THC** are not differentiated, but otherwise, the performance of this minimal sensor is strong. Importantly, when the **1•2•M** data is processed using Linear Discriminant Analysis (Figure S-13), complete discrimination is possible. This treatment is statistically valid, but as the results are pre-sorted into groups before analysis, it is a less optimal method for analyzing unknowns than the unbiased PCA. As the hydrophilic metabolites **11-COOH-THC** and **11-OH-THC** are the desirable targets for urinalysis in an unknown sample, PCA is the preferable analysis method. Fortunately, adding the **1•3•M** results to the array introduces sufficient additional variables to allow differentiation of **11-COOH-THC** and **11-OH-THC**, as shown in Figure 3c. A third principal component is required, but selectivity for all six metabolites is possible.

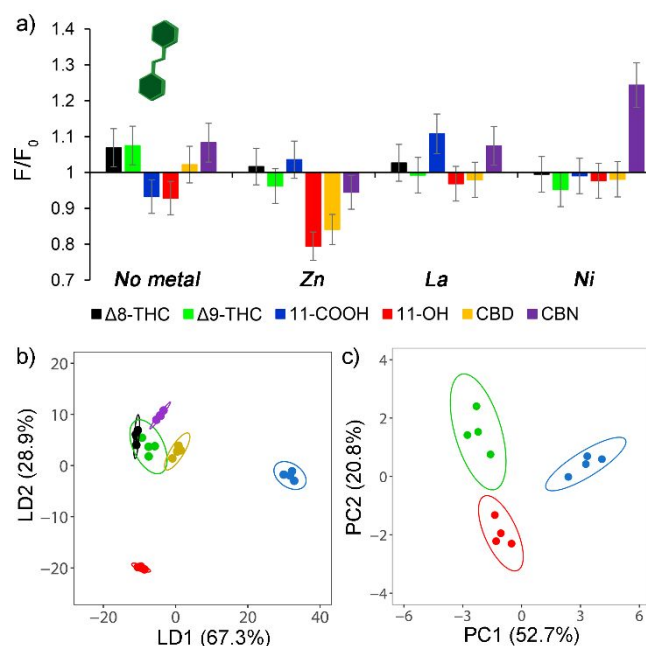


Figure 4. a) Fluorescence responses of the 6 different THC metabolites with guest **2** in pooled human saliva. [1] = 20 μ M; [2] = 1.5 μ M; [M^{2+}] = 50 μ M; [THC metabolite] = 30 μ M; b) LDA scores plot for all 6 THC metabolites; c) PCA scores plot for Δ^9 -THC, **11-OH-THC** and **11-COOH-THC**. Both plots use an 11-factor array with **1•2** or **1•3** and either no metal or 50 μ M Zn^{2+} , Cu^{2+} , Ni^{2+} , Cd^{2+} , La^{3+} or Ca^{2+} . Ellipses determined at 95% confidence.

The sensor arrays were then tested in commercial human saliva, using the same analysis method as before in urine (Figure 4). Saliva proved to be even more challenging a medium than urine, however, and the minimal arrays (**1•2•M** or **1•3•M**) were not successful in discriminating between all six metabolites, by either LDA or PCA. Combination of both fluorophores in the array did allow some selectivity in sensing,

with the hydrophilic **11-COOH-THC** and **11-OH-THC** fully separated from the more hydrophobic targets. Separation of the highly similar targets was unsuccessful in saliva, but it is important to note that the desired target of THC testing is to selectively discriminate Δ^9 -THC from its metabolites. The sensor array is well-capable of discriminating between Δ^9 -THC, **11-COOH-THC** and **11-OH-THC** in the scores plot. While the array cannot distinguish between isomers like Δ^9 -THC and Δ^8 -THC, it is more than capable of detecting the biorelevant targets in μM concentrations in saliva, as well as urine.

While the whole array can selectively sense and discriminate THC targets in multiple different biofluids, different components have different efficacy in different fluids, leading to the question of which specific components are most effective, and why. The affinity of **1** for hydrophobic guests is relatively constant in different media,¹¹ so the variations in performance are likely due to variations in forming host:dye:metal complexes that can allow optical detection. It is clear that the sensing is most effective in urine, rather than saliva, and that the host:guest complex **1•2** retains its performance in biofluids better than the **1•3** complex (relative to that in aqueous solution). The fluorescence response of **1•2**, **1•2•La³⁺** and **1•3** was tested in pure water, Tris buffer, urine and saliva (see ESI). For guest **3**, quenching upon binding in **1** is far stronger in Tris than in water, but is significantly reduced in both saliva and urine. In addition, the effect of adding 50 μM La³⁺ is vastly reduced in high salt biofluids. Guest **2** is quite different, as the fluorescence enhancement upon forming the **1•2** complex is actually *increased* in urine and saliva with respect to that in water or Tris. The constituents of the respective biofluids explain these differences. The major component of urine^{5c} is obviously urea (13.4 g/L), accompanied by other small organics such as amino acids, creatinine and hippurate, and inorganic salts such as NaCl, KCl, K₂SO₄, with a total concentration $\sim 14\text{g/L}$. Saliva, on the other hand, has a relatively high proportion of cationic proteins, including mucins and acidic proline-rich proteins (PRPs).^{5b} The sensing performance of **1•3** has been shown to be unaffected by amino acids up to mM concentrations,^{3d} but high salt conditions can prevent the triggered aggregation of the **1•3** complex, and thus the fluorescence quenching. This requirement for aggregation limits the performance of **1•3** in biofluids. Fortunately, guest **2** does not require aggregation for fluorescence, and so the **1•2** complex is formed strongly in all media. The limiting factor is not the dye, but the coordination of the heavy metal salts, which is understandably lessened (although importantly *not prevented*) in high salt media. The major issue in saliva is the presence of cationic proteins, to which both **1•2** and **1•3** are quite sensitive. Despite that, THC metabolite discrimination with the sensor is still effective, further illustrating the power of the relatively simple, yet highly versatile deep cavitated host.

The authors would like to thank the National Science Foundation (CHE-1707347 to WZ and RJH) for support.

Conflicts of interest

There are no conflicts to declare.

Notes and references

- a) F. Hof, *Chem. Commun.*, 2016, **52**, 10093; b) J. E. Beaver, M. L. Waters, *ACS Chem. Biol.* 2016, **11**, 643; c) S. J. Barrow, S. Kaser, M. J. Rowland, J. del Barrio, O. A. Scherman, *Chem. Rev.*, 2015, **115**, 12320; d) S. Dasgupta, P. S. Mukherjee, *Org. Biomol. Chem.*, 2017, **15**, 762; e) J. H. Jordan, B. C. Gibb, *Chem. Soc. Rev.*, 2015, **44**, 547.
- a) S. van Dun, C. Ottmann, L.-G. Milroy, L. Brunsveld, *J. Am. Chem. Soc.*, 2017, **139**, 13960; b) G. Ghale, W. M. Nau, *Acc. Chem. Res.*, 2014, **47**, 2150; c) R. Pinalli, A. Pedrini, E. Dalcanale, *Chem. Soc. Rev.*, 2018, **47**, 7006.
- a) I. Lazar, F. Biedermann, K. R. Mustafina, K. I. Assaf, A. Hennig, W. M. Nau, *J. Am. Chem. Soc.*, 2016, **138**, 13022; b) B. C. Peacor, C. M. Ramsay, M. L. Waters, *Chem. Sci.*, 2017, **8**, 1422; c) S. A. Minaker, K. D. Daze, M. C. F. Ma, F. Hof, *J. Am. Chem. Soc.*, 2012, **134**, 11674; d) Y. Liu, L. Perez, M. Mettry, C. J. Easley, R. J. Hooley, W. Zhong, *J. Am. Chem. Soc.*, 2016, **138**, 10746; e) Y. Liu, L. Perez, M. Mettry, A. D. Gill, S. R. Byers, C. J. Easley, C. J. Bardeen, W. Zhong, R. J. Hooley, *Chem. Sci.*, 2017, **8**, 3960.
- L. You, D. Zha, E. V. Anslyn, *Chem. Rev.* 2015, **115**, 7840.
- a) S. P. Humphrey, R. T. Williamson, *J. Prosthet. Dent.*, 2001, **85**, 162; b) L. C. Schenkels, E. C. Veerman, A.V. Nieuw Amerongen, *Crit. Rev. Oral Biol. Med.* 1995, **6**, 161; c) D. F. Putnam, *NASA Contractor Report CR-1802*, 1971.
- a) A. Norouzy, Z. Azizi, Z.; W. M. Nau, *Angew. Chem., Int. Ed.*, 2015, **54**, 792; b) Y.-J. Ghang, M. P. Schramm, F. Zhang, R. A. Acey, C. David, E. H. Wilson, Y. Wang, Q. Cheng, R. J. Hooley, *J. Am. Chem. Soc.*, 2013, **135**, 7090.
- a) T. Minami, N. A. Esipenko, A. Akdeniz, B. Zhang, L. Isaacs, P. Anzenbacher, *J. Am. Chem. Soc.*, 2013, **135**, 15238; b) E. G. Shcherbakova, B. Zhang, S. Gozem, T. Minami, P. Y. Zavalij, M. Pushina, L. Isaacs, P. Anzenbacher, *J. Am. Chem. Soc.*, 2017, **139**, 14954; c) S. Sinn, E. Spuling, S. Bräse, F. Biedermann, *Chem. Sci.*, 2019, **10**, 6584.
- a) G. A. Garnett, K. D. Daze, J. A. Pena Diaz, N. Fagen, A. Shaurya, M. C. Ma, M. S. Collins, D. W. Johnson, L. N. Zakharov, F. Hof, *Chem. Commun.*, 2016, **52**, 2768; b) M. A. Beatty, A. T. Pye, A. Shaurya, B. Kim, A. J. Selinger, F. Hof, *Org. Biomol. Chem.*, 2019, **17**, 2081.
- a) M. A. Beatty, J. Borges-González, N. J. Sinclair, A. T. Pye, F. Hof, *J. Am. Chem. Soc.*, 2018, **140**, 3500; b) M. A. Beatty, A. J. Selinger, Y. Li, F. Hof, *J. Am. Chem. Soc.*, 2019, **141**, 16763.
- a) R. S. Niedbala, K.W. Kardos, D. F. Fritch, S. Kardos, T. Fries, J. Waga, J. Robb, E. J. Cone, *J. Anal. Toxicol.*, 2001, **25**, 289; b) J. Röhrich, I. Schimmel, S. Zörntlein, J. Becker, S. Drobnik, T. Kaufmann, V. Kuntz, R. Urban, *J. Anal. Toxicol.*, 2010, **34**, 196; c) K. Watanabe, S. Yamaori, T. Funahashi, T. Kimura, I. Yamamoto, *Life Sci.*, 2007, **80**, 1415. d) M. A. Huestis, J. M. Mitchell, E. J. Cone, *J. Anal. Toxicol.*, 1996, **20**, 441. e) G. Milman, D. M. Schwoppe, D. A. Gorelick, M. A. Huestis, *Clin Chim Acta*, 2012, **413**, 765.
- R. J. Hooley, H. J. Van Anda, J. Rebek, Jr., *J. Am. Chem. Soc.*, 2007, **129**, 13464.
- A. D. Gill, L. Perez, I. N. Q. Salinas, S. R. Byers, Y. Liu, B. L. Hickey, W. Zhong, R. J. Hooley, *Chem-Eur. J.* 2019, **25**, 1740.
- Y. Liu, M. Mettry, A. D. Gill, L. Perez, W. Zhong, R. J. Hooley, *Anal. Chem.*, 2017, **89**, 11113.
- P. C. Jurs, G. A. Bakken, H.E. McClelland, *Chem. Rev.* 2000, **100**, 2649.
- L. Trembleau, J. Rebek, Jr. *Science*, 2003, **301**, 1219.